Informatics in Medicine Unlocked 13 (2018) 133–138

Contents lists available at ScienceDirect

Informatics in Medicine Unlocked

journal homepage: www.elsevier.com/locate/imu

Abnormality recognition and feature extraction in female pelvic ultrasound imaging

Lidiya Thampi [a,*], Varghese Paul [b]

[a] Department of Information Technology, Cochin University of Science and Technology, India
[b] Department of Information Technology, Rajagiri School of Engineering and Technology, India

ARTICLE INFO

Keywords:
Speckle
Segmentation
Tumor
Feature extraction and ultrasound imaging

ABSTRACT

The detection of uterine abnormalities in the early stage is challenging and it aims to play a vital role in automated screening systems. The algorithm proposed herein works in the following way: initially a PDE (Partial Differential Equation approach) based speckle reduction is carried out in a preprocessing stage, and the region of interest is separated from the female pelvic ultrasound images. Then the texture and shape features are extracted from the segmented ROI component. The results of shape similarity indices between manual and automated segmentations are also illustrated. The simulation result analysis of this algorithm was implemented in MATLAB R2016a. In this paper, an automatic segmentation scheme is proposed which will aid the radiologists for better outputs in very limited time making the proposed solution very effective and productive.

1. Introduction

The burden of cervical cancer is expected to rise worldwide, particularly in low and middle income countries (LMICs) like India and China. India, the second most populous country in the world, presently has 1.34 billion people, and is predicted to have more than 1.53 billion people by the end of 2030. The number of new cases of cancer deaths (cancer mortality) at different age group is shown in Fig. 1. Most cases occur between the ages of 50 and 60 years. The risk of developing cancer is also expanding with the increase in population growth. Ultrasound imaging is a common modality used in many diagnostic and therapeutic applications which aims to provide early detection of tissue characteristics.

Nowadays, more ongoing projects are presented and are being developed for analysing the disorder of tumor-like structures. These computer aided diagnosis (CAD) systems assist doctors in recognising the abnormal areas, but there are still complexities arising from the low contrast, high amount of speckle and low signal to noise ratio circumstances present in ultrasound B-scan images [1]. Transvaginal ultrasound follows with the physical examination in diagnosing pelvic ultrasound (PUS) imaging. If anything unusual is detected in the ultrasound, the patient is referred for a surgical biopsy or Pap smear test, as these will assist to examine the cell changes readily.

The remainder of the paper is organized as follows. Section 2 presents the relative work proposed by different researchers. Section 3 describes the implementation of CAD system and the performance evaluation, and results and discussion are provided in sections 4 and 5, and finally conclusions are given in Section 6.

2. Related work

Several imaging modalities like transvaginal ultrasonography (TVUS), computed tomography (CT), and magnetic resonance imaging (MRI) have been used as a diagnostic tool for the pre-treatment work-up of cervical cancer all over the world [2,3]. Alcazar et al. [3] described that the role of ultrasound imaging was increased for assessing the PUS, while MRI is commonly used for local extent of disease evaluation, and PET scan for distant evaluation. If the ultrasound cancer detection provides greater accuracy, then unnecessary surgical biopsies can be avoided [4]. Therefore, ultrasound imaging is preferable in large-scale screening programmes because of its cost effectiveness and lesser radiation effect.

A well-experienced radiologist can easily elucidate PUS images and thereby determine the diagnosis effectively. Segmentation plays a key role in computational processing of medical images. Since the medical images are highly corrupted with noise, a fully segmented algorithm is indispensable to visualise the relative position and shapes of internal tissue.

Kass et al. [6] initially proposed the massively used edge segmentation method called active contour model or snakes. A few algorithms are

* Corresponding author.
E-mail address: lidiyarijo@cusat.ac.in (L. Thampi).

https://doi.org/10.1016/j.imu.2018.02.005
Received 15 December 2017; Received in revised form 16 January 2018; Accepted 20 February 2018
Available online 23 February 2018

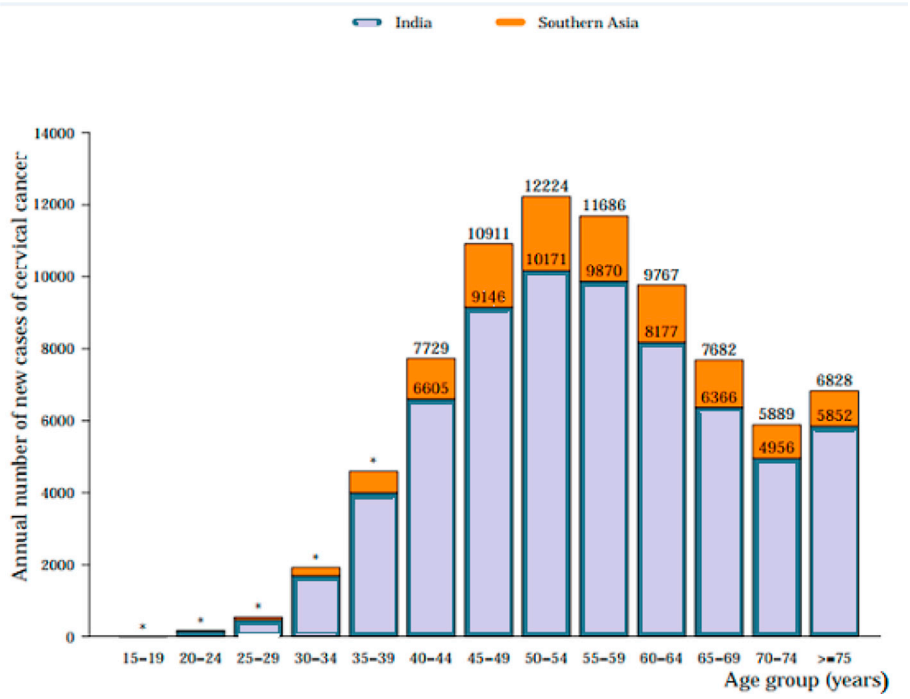

Fig. 1. Annual number of death cases of cervical cancer by age group in India. Summary report 27 July 2017). (Adapted from C. Bruni L et al. [5]).

developed by many from these basic segmentation methods. Selvathi et al. [7] have made an attempt to extract the local properties of ultrasound kidney images. The concept was based on regularized level set evolution which is an active contour based segmentation. S.G. Antunes et al. [8] also proposed an active contour model based on phase symmetry and level set evolution for the segmentation of echocardiography images. Here the algorithm can simultaneously extract all heart cavities in fully automatic way. Li et al. [9] have evaluated different intensity based methods on regular kidney contour images and phantom kidney images. The study shows that algorithms are effective only for homogeneous image features rather than heterogeneous lesions.

R.-F. Chang et al. [10] used a threshold method based on histogram approximation to separate the tumor region from the background image. The method was adapted from Ref. [11]. He found out the threshold value by minimizing the sum-of-square errors SSE (t) between the grey values and the mean values in the two regions. A new approach is proposed by Ahror Belaid et al. [12] to extract the left ventricle boundaries using phase based level set. He uses a new speed term based on local phase and local orientation derived from the monogenic signal. Also Cauchy functions are used rather than traditional log-Gabor function for the feature extraction.

In this paper, we proposed a segmentation method based on morphological marker controlled watershed segmentation to identify lesion region. The segmentation results are compared with those provided by the active contour based [6], level set based [12], thresholding based [11] and watershed methods.

3. Implementation of CAD system

The functional block diagram of proposed work is shown in Fig. 2. The transducer attached to the scanner uses high frequency sound waves (in the range of 3–7 MHz) to create ultrasound image of the body tissues. Analysis of region of interest in noisy nature is very crucial as these real time ultrasound images can be used as a good tool for guiding other invasive procedures.

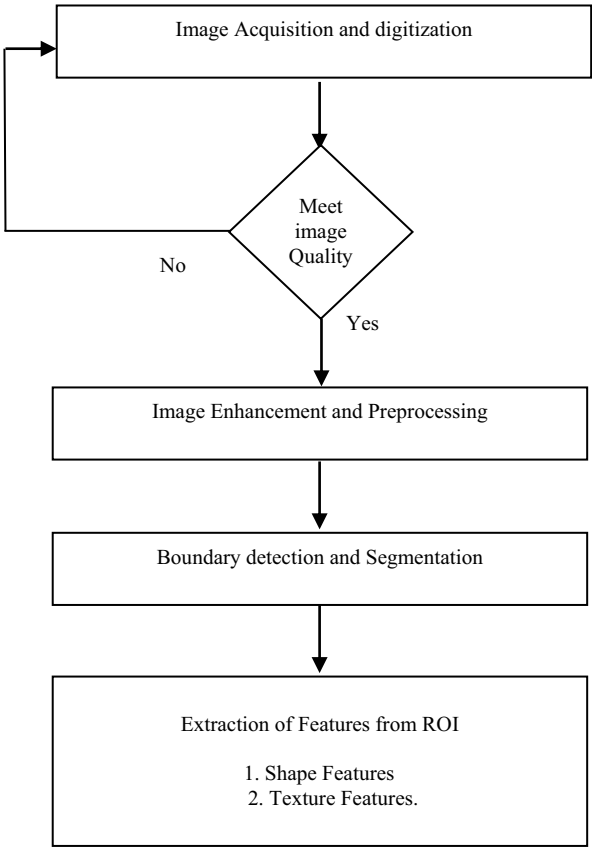

Fig. 2. CAD system.

3.1. Preprocessing

If the digitized medical image meets the quality, then image enhancement or preprocessing is carried out. Speckle, a form of multiplicative noise commonly seen in medical ultrasound images effects the image edges and makes the diagnostic interpretation difficult. So it's important to remove speckle without destroying the important image features. Many adaptive and Non-adaptive filters have been used earlier, in that the most widely cited applied filters include Lee, Kuan, Frost and Median filters [see 13–15]. Although the existing despeckle filters have the advantage of edge preserving, but they are subjected to some major limitations. So a PDE (partial differential equation approach) based speckle reducing anisotropic diffusion filter is proposed in Ref. [16]. Filter comparison of the given filter with Lee and Kuan [17] is shown in Fig. 3. This adaptive SRAD filter is independent of using hard thresholds to alter the performance of edges. The diffusion technique used here is an extension of [13] [14] which is based on minimum mean square error (MMSE) design approach. The above anisotropic diffusion method is build from a non-linear PDE for smoothening the speckle effected image data.

$$\left\{ \begin{array}{l} \dfrac{\partial S(i,j;t)}{\partial t} = div[d(x)\nabla(S(i,j;t))] \\ S(t=0) \rightarrow S(i,j;0) = S_0(i,j) \end{array} \right\} \quad (1)$$

S (i, j; t) is the output image obtained from the input intensity image *S_0 (i, j)* respectively.

$$d(x) = \frac{1}{1 + [x^2(i,j;t) - x_0^2(t)]/[x_0^2(t)(1 + x_0^2(t)]} \quad (2)$$

d(x) is the diffusion coefficient and *x(i,j;t)* is the instantaneous coefficient of variation. The latter is a function of local gradient magnitude and Laplacian operator to act like a good edge detector.

$$x(i,j;t) = \sqrt{\frac{((1/2)(|\nabla S|/S^2) - (1/16)(\nabla^2 S/S)^2)}{[1 + (1/4)(\nabla^2 S/S)]^2}} \quad (3)$$

$$x_0(t) \approx x_0 \exp(-t) x_0(t) \approx x_0 \exp(-\rho t) \quad (4)$$

In order to reduce the exponential decay rate, a single constant ρ (value < 1) is introduced in the speckle scale function $x_0(t)$in the above equation. Also the speckle coefficient of variation $x_0$is assumed to be 1 for ultrasound image data. The preprocessed output with time step $\Delta t = 0.02$ per iteration is shown in Fig. 4.

3.2. Segmentation

The earliest systems have mostly relied upon the traditional methods of image segmentation which is confined to the basic edge based and region based segmentation techniques. The edge detection is very sensitive to noise and artefacts and it badly affects the edge detector for proper boundary extraction. The frequently used region based algorithms is a solution to this, in this paper morphological marker controlled watershed algorithm is used (MMCW).

It can be difficult to delineate the tumor margins on ultrasound images. Most of the algorithms depend upon some basic assumption related to tumor intensity, shape and position. Since the image structure is different for diverse ultrasound images, algorithms based upon these primary assumptions is not enough for doing further operations. So an automatic segmentation scheme should be adopted for analysing the lesion region. Fig. 4 shows the PUS imaging (endometrial adenocarcinoma) with central mass appeared as white region.

3.2.1. Morphological marker-controlled watershed segmentation (MMCW)

Our main aim is to separate the tumor region from PUS images without any human control. So the SRAD based filtered image is subjected to basic grey scale morphology for getting a smoothing effect on MMCW segmentation [18]. The change in intensity of each pixel can be easily measured using image gradient. The method starts with gradient magnitude as a segmentation function. The direct application of watershed transform results in over segmentation problem (large number segmented regions) and this severe segmentation can be controlled by incorporating the concept of markers.

Internal (foreground) and external (background) markers form the connected component of an image. Internal markers are associated with region of interest which is seen as blob like regions inside the foreground objects. In this paper opening-by-reconstruction and closing-by-reconstruction morphological techniques are used for tracking the internal markers. Regional maxima of these foreground objects is calculated for getting a smoothening edge. For a better representation of resultant image, the foreground markers are superimposed on original image. For computing the background markers thresholding method is initialized. Then for thinning the unwanted black background pixels watershed transform of the distance transform is computed. Finally the watershed based segmentation is applied to modified gradient image to obtain the desired segmented objects. Fig. 5 shows the stage by stage results of endometrial adenocarcinoma.

3.3Algorithm

- Converted gray scale image is filtered by SRAD filter.
- Erosion is done for smoothening purpose.
- Develop the gradient image using sobel edge mask.
- Incorporating the concept of internal and external markers.
- Start with marking foreground objects using opening closing by reconstruction.
- Calculating regional maxima
- Superimposing the modified regional maxima on the original image
- Thresholding is done for computing background markers.
- Compute watershed based segmentation.
- Finally superimposing both markers and object boundaries on original image to get the tumor part.

3.4. Extraction of multiple features from selected ROI

The final stage of proposed CAD system focuses on extraction of multiple features from the selected region of interest (ROI). The optimal features can be selected from these multiple ROI features for proper

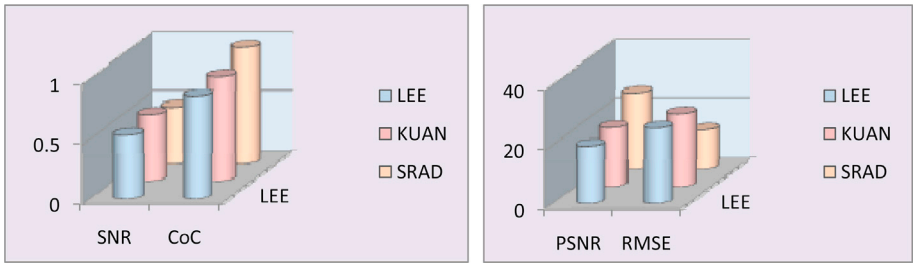

Fig. 3. Filter comparisons for Lee, Kuan and SRAD

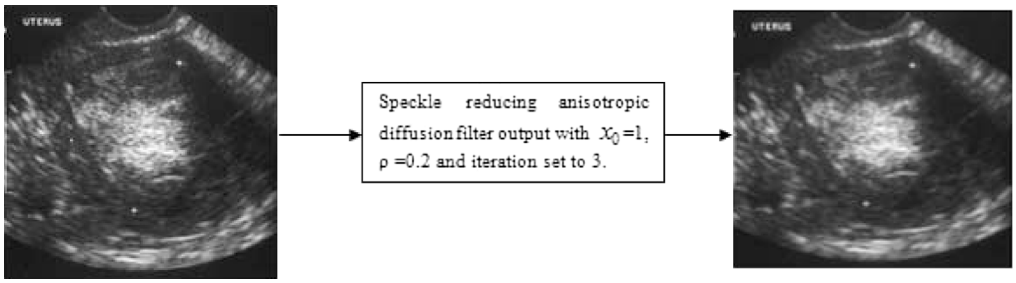

Fig. 4. Output of the preprocessed image.

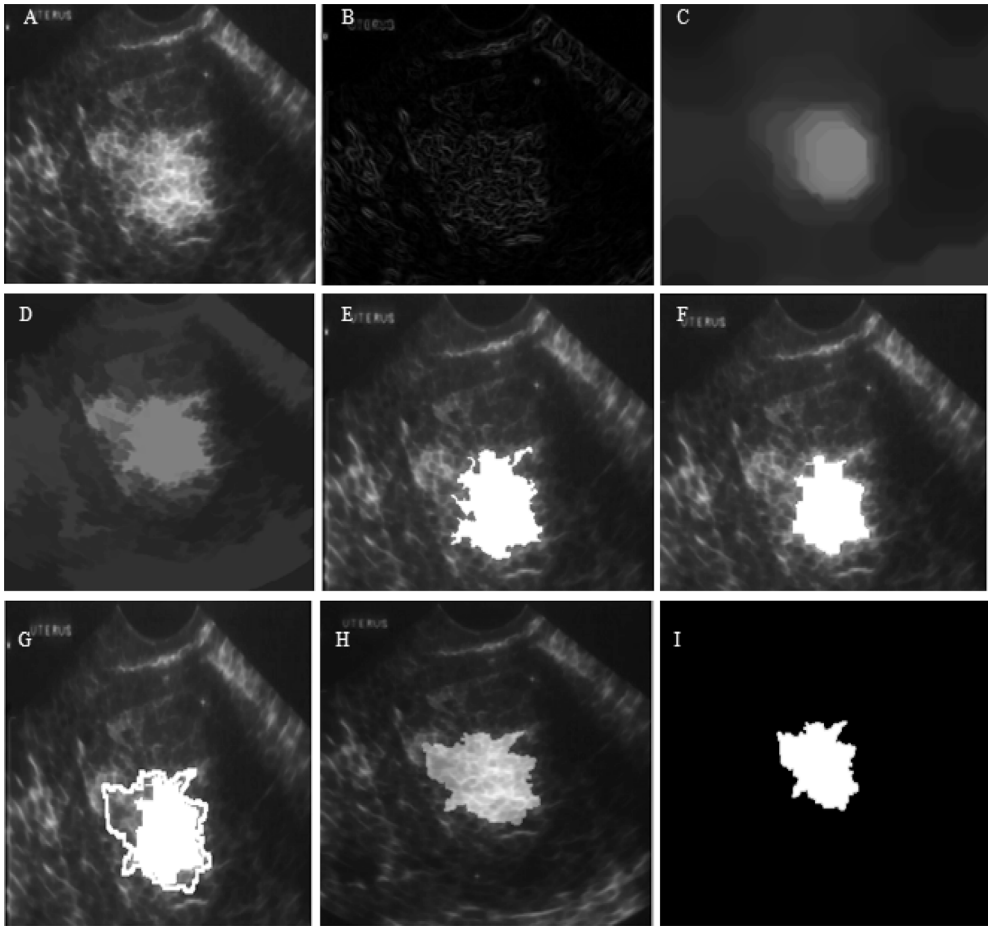

Fig. 5. Segmentation image outputs. **A**. SRAD filtered image after erosion **B**. Gradient image **C**. Opening-closing **D**. Opening-closing by reconstruction **E**. Regional maxima **F**. Modified regional maxima superimposed on original image **G.** Markers and object boundaries of region of interest **H.** Applying coloured label to final contour **I**. Identified tumor separated.

classification of tumor part (considering only in future work). In this study, two categories of PUS image features are presented which includes shape and texture features. Shape is one of the important observing criteria used for classifying the lesions in ultrasound images [18]. In this work the most frequently used 8 shape parameters like area (FE_1), perimeter (FE_2), major axis and minor axis length (FE_3), centroid (FE_4), equidiameter (FE_5), solidity (FE_6), circularity ratio (FE_7) & eccentricity (FE_8) are included. Similarity of the required region to a circle is described by its circularity ratio and to a convex or concave is given by solidity.

$$CircularityRatio = \frac{4\pi \times Area}{Perimeter^2} \tag{5}$$

$$Solidity = \frac{Area}{Convexhull \quad Area} \tag{6}$$

Area specifies the number of (non zero) pixels in the tumor region whereas perimeter specifies the distance around the boundary of that region.

Equidiameter is given by,

$$Equidiameter = sqrt\left(4\pi \times \frac{Area}{pi}\right) \tag{7}$$

The eccentricity characterizes to the un-circularity of ROI. It is given by,

$$Eccentricity = \frac{distance\ between\ the\ foci}{major\ axis\ length} = \frac{\sqrt{a^2 - b^2}}{a} \tag{8}$$

where a and b represents the semi-major and semi-minor axis length. In addition to this structure based features, texture features are also presented for discriminating the tumor from normal tissues. Total ten textural features (FE_9 to FE_18) are measured from the grey level co-occurrence matrix c(x). In that angular second moment, correlation,

sum of squares: variance, entropy, inverse difference, contrast, difference variance, difference entropy, information measure of correlation 1, and information measure of correlation 2 are considered for diagnosis of data which is defined by Haralick et al. [20].

4. Quality assessment

The similarity check process involves in verification of manual segmented region with the contour of extracted region. The manual segmentation process would involve in segmenting the cancer region in the ultrasound images manually over the images. The manual segmented data would be stored separately and later compared with the achieved segmentation results for computing the similarity metrics.

For brevity the similarity measures was carried out on six ultrasound images which is reviewed and validated with the aid of radiologists. Similarity index refers to ratio of true positive pixel element number to the sum of automated and manual pixel element numbers. Jaccard similarity index and Dice similarity coefficient or (Zijdenbos similarity index) are used to calculate the similarity and diversity of manually *versus* automated segmentations. Both are equivalent but ZSI is commonly used in image segmentations.

$$SI = \frac{2^{*}Truepositi\ ve_{PixelNumber}}{Manual_{PixelNumber} + Automated_{PixelNumber}} \tag{9}$$

$$JSI = \frac{Manual_{Segmentation} \cap Automated_{Segmentation}}{Manual_{Segmentation} \cup Automated_{Segmentation}} \tag{10}$$

$$DSC = \frac{2^{*}(Manual \cap Automated)_{Segmentation}}{Manual_{PixelNumber} + Automated_{PixelNumber}} \tag{11}$$

The values of true positive (TP), false positive (FP), true negative (TN) and false negative (FN) are also noted to calculate the *False positive rate or fall-out (FPR)* $= FP/(FP + TN)$ and False *negative rate (FNR)* $= FN/(FN + TP)$.

5. Results and discussion

The proposed system assists in detecting the abnormalities present in pelvic ultrasound imaging systems. The simulation result analysis was carried out in MATLAB R2016a. The sample image has been pre-processed using SRAD filter. The performance comparison of the above filter with other filters is shown in Fig. 3. It is seen that the SRAD filter performs well. The sample input image and its corresponding output, along with the details, is given in Fig. 4. It is to be also noted that a constant ρ value of 0.2 is introduced to avoid the decay rate of the speckle scale function.

The pictorial representation of algorithm in different stages is given in Fig. 5. It is shown that the identified tumor is clearly separated in Fig. 5 (H & I). Fig. 6 presents the segmentation results of 3 PUS images. Also, over-segmentation problem of three images can be seen clearly in Fig. 6 c. The introduction of internal and external markers forms a distinction in effortless tumor identification.

From the results it can be clearly observed that the proposed CAD system can able to segment the tumor with different sizes and shapes. T1 and T3 are irregular shape contours whereas T2 is nearly an oval shape tumor. Due to the intensity difference of T2 from T1 and T3, algorithm wrongly segments two contours (Fig. 6 d.) is one of the limitations of the proposed approach. The final contour outlined by green colour label as shown in Fig. 6 d.

The texture and shape features were estimated from the segmented region of interest. Total 18 features were extracted. The obtained range of values for diverse ultrasound images is illustrated in Table 1. The results of three shape similarity indices between manual and automated segmentations can be seen in Table 2. The comparison result gives an average similarity index of 82.65% and JSI of 76.5% and a DSC of 83.8%. The proposed method achieved a good similarity result and JSI value when compared to 74.5% obtained in Ref. [21]. In addition the system also got an average false positive rate which is less than 0.05 and an average false negative rate of 0.18 which is acceptable when compared

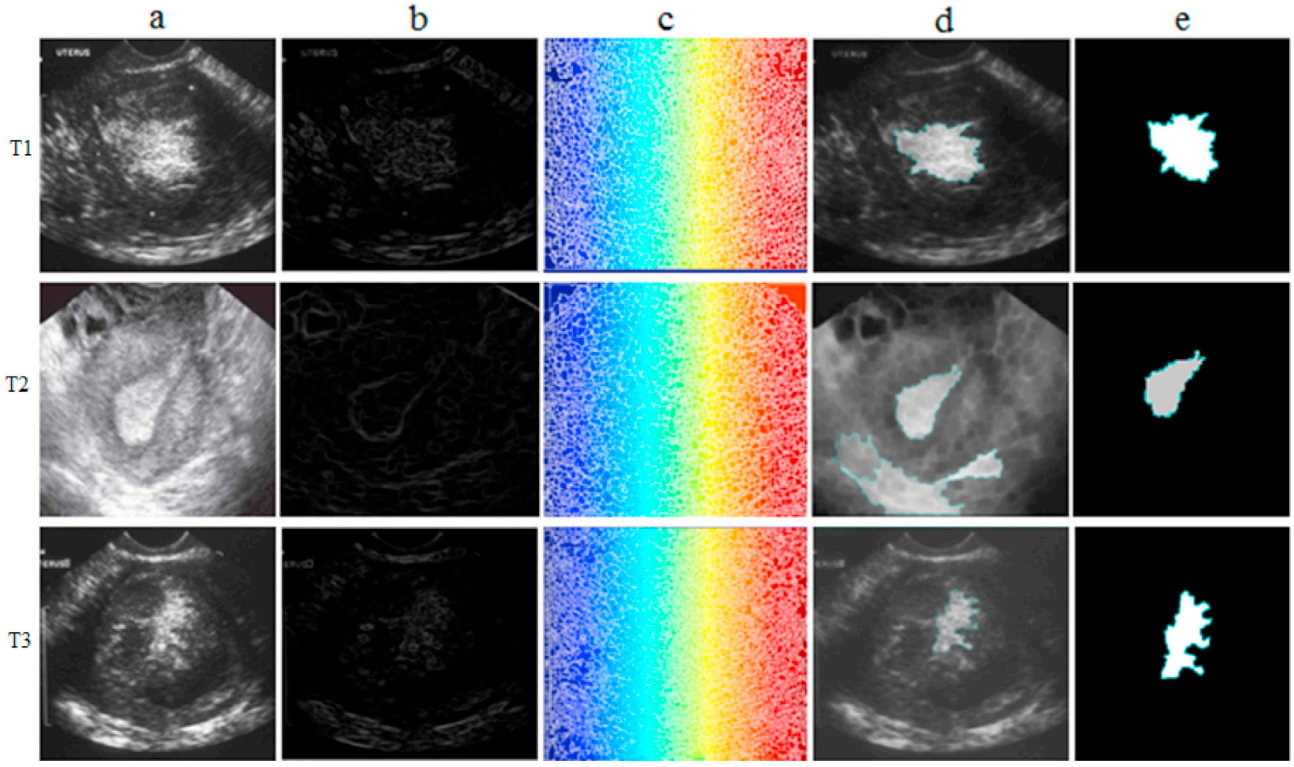

Fig. 6. Segmentation results of three PUS tumor image samples. Column 'a' shows the three input images T1, T2, T3. Column 'b' its gradient image outputs. Column 'c' over-segmentation problem. Column 'd' final contour. Column 'e' separated ROI part.

Table 1
Details of extracted shape and textural features.

Feature Category	Feature Description	Range of Values
Shape Feature	FE_1: Area	2755–4917
	FE_2: Perimeter	546–1073
	FE_3: Major axis and Minor axis length	64–118.11; 76.2–119.5
	FE_4: Centroid	130,137–243, 170
	FE_5: Equidiameter	59.23–79.12
	FE_6: Solidity	0.732–0.923
	FE_7: Circularity	0.054–0.17
	FE_8: Eccentricity	0.32–0.672
Textural Features [20]	FE_9: Angular second moment	0.901–0.972
	FE_10: Correlation	882.08–3.26e+03
	FE_11: Sum of Squares: Variance	903.2–3.33e+03
	FE_12: Inverse Difference	0.93–0.998
	FE_13: Entropy	0.08–0.2153
	FE_14: Contrast	42.24–179.52
	FE_15: Difference variance	0.0019–0.002
	FE_16: Difference entropy	−0.006–−0.0192
	FE_17: Information measure of correlation 1	−0.915 - – 0.94
	FE_18: Information measure of correlation 1	0.36–0.56

Table 2
Comparison of manual segmentation and automated segmentation using similar metrics.

Test Image	I1	I2	I3	I4	I5	I6	Average
SI (%)	87.8	92.5	80.5	78.3	75.6	81.2	82.7
JSI (%)	78.1	86.2	67.7	71.5	73.9	82.1	76.5
DSC (%)	87.2	92.5	80.6	83.4	79.2	80.4	83.8

with a *FPR and FNR* value of radiologists assessment (0.35 *and* 0.11) and the proposed method (0.04 *and* 0.08) in Ref. [22].

6. Conclusion and future work

Due to the complexities arising from the low contrast, high speckle ratio and low SNR, computer-aided diagnosis systems are absolutely necessary for analysing the lesions in ultrasound images. In this paper, an automatic segmentation scheme was proposed, which will aid the radiologists for better outputs in a limited time frame. Firstly, the speckle reduced anisotropic diffusion filter is used as a preprocessing approach. Furthermore, morphological marker controlled watershed segmentation is applied to identify the lesion region. Then a total of 18 features are extracted including shape and textural components. Finally the method is compared with manual drawing in order to evaluate the performance.

Because of the high dynamic range of received sound waves in ultrasound imaging, various global and local compression techniques were studied as a replacement for logarithmic methods [23]. This will be assistive to transmit the scanned images from the patients to a cloud-based storage, so that the doctors can access the data and carry out the diagnosis in a limited time duration. An FPGA (Xilinx Kintex 7) based CAD algorithm is implemented for discriminating cysts and stones in kidney ultrasound images [24]. A look-up table based approach used here is helpful in differentiating normal and abnormal images. A bicluster score optimal feature selection is employed in Ref. [19] to select 25 features from a total of 73 features. These might be implemented in our system in future work.

The proposed method can be extended to classification by extracting a maximum number of features. Also, stage-by-stage prediction (cysts, fibroids) [25] of tumors is possible via a supervised classification output. It is important to train the algorithm with a maximum number of input images for achieving an improved result. The initial staging diagnosis may be suggested for better verification and to detect any suspected problems.

Conflicts of interest

The authors declare no conflict of interest.

Acknowledgements

The authors would like to thank the principal, faculty members and the research scholars of IT (Information Technology) Department for their sincere support and effort for this research work. This research did not receive any specific grant from funding agencies in the public, commercial, or not-for-profit sectors. The ultrasound images are downloaded from Google.com/images.

References

[1] Burckhardt CB. Speckle in ultrasound B-mode scans. IEEE Trans Son Ultrason 1978; SU-25(1):1–6.
[2] Faria S.C, et al. Imaging in endometrial carcinoma. Indian J Radiol Imag 2015; 25(2):137–47.
[3] Alcázar JL, et al. The role of ultrasound in the assessment of uterine cervical cancer. J Obstet Gynaecol India 2014;64(5):311–6.
[4] Cheng HD, et al. Automated breast cancer detection and classification using ultrasound images: a survey. Pattern Recogn 2010;43(1):299–317.
[5] Bruni L, Barrionuevo-Rosas L, Albero G, Serrano B, Mena M, Gómez D, Muñoz J, Bosch FX, de Sanjosé S. Human papillomavirus and related diseases in India, ICO information centre on HPV and cancer (HPV information centre), vol. 27; July 2017. Summary Report.
[6] Kass M, et al. Snakes: active contour models. Int J Comput Vis 1988;1(4):321–31.
[7] Selvathi D, Bama S. Phase based distance regularized level set for the segmentation of ultrasound kidney images. Pattern Recogn Lett 2017;86:9–17.
[8] Antunes SG, et al. "Phase symmetry approach applied to children heart chambers segmentation: a comparative study. IEEE Trans Biomed Eng 2011;58(8).
[9] Li, et al. A comparative study of ultrasound image segmentation algorithms for segmenting kidney tumors. In: Proc. 4th int. Symp. Appl. Sci. Biomed. Commun. Technol. - ISABEL '11; 2011. p. 1–5.
[10] Chang R-F, et al. Segmentation of breast tumor in three-dimensional ultrasound images using three-dimensional discrete active contour model. Ultrasound Med Biol 2003;29(11):1571–81.
[11] Ramesh N, et al. Thresholding based on histogram approximation. IEE Proc Vis Image Signal Process 1995;142(5):271–9.
[12] Belaid A, et al. "Phase-Based level set segmentation of ultrasound images. IEEE Trans Inf Technol Biomed 2011;15(1):138–47.
[13] Lee JS. "Digital image enhancement and noise filtering by using local statistics. IEEE Trans Pattern Anal Mach Intell 1980;PAM1–2.
[14] Kuan DT, Sawchuk AA, Strand TC, Chavel P. "Adaptive restoration of images with speckle. IEEE Trans Acoust Speech Signal Process 1987;ASSP-35:373–83.
[15] Loupas T, et al. "An adaptive weighted median filter for speckle suppression in medical ultrasonic images". IEEE Trans Circ Syst 1989;36(1):129–35.
[16] Yongjian Y, et al. Speckle reducing anisotropic diffusion. IEEE Trans Image Process 2002;11(11).
[17] Thampi LL, et al. An automatic segmentation of endometrial cancer on ultrasound images. IEEE Inter .Con. Comm. Signal Processing 2013:139–43.
[18] Parvati K, et al. Image segmentation using gray-scale morphology and marker-controlled watershed transformation. Hindawi Discrete Dynamics in Nature and Society 2008.
[19] Huang Q, Yang F, Liu L, Li X. Automatic segmentation of breast lesions for interaction in ultrasonic computer-aided diagnosis. Inf Sci 2015;314:293–310.
[20] Haralick R, et al. "Textural features for image classification. IEEE Trans. Systems, Man and Cybernetics 1973;3:610–21.
[21] Gu Peng, et al. Automated 3D ultrasound image segmentation to aid breast cancer image interpretation. Ultrasonics 2016;65:51–8.
[22] Shi Xiangjun, et al. Detection and classification of masses in breast ultrasound images. Digit Signal Process 2010;20(3):824–36.
[23] Akkala V, et al. Compression techniques for IoT enabled handheld ultrasound imaging system. 2014 IEEE Conf. Biomed. Eng. Sciences. 2015:648–52.
[24] Divya Krishna K, et al. Computer aided abnormality detection for kidney on FPGA based IoT enabled portable ultrasound imaging system. Irbm 2016;37(4):189–97.
[25] Sahdev, Reznek RH. Magnetic resonance imaging of endometrial and cervical cancer. Ann N Y Acad Sci 2008;1138:214–32.